EXPERIMENTAL INVESTIGATION OF NANOCOMPOSITE MATERIALS JOINED BY FRICTION WELDING FOR BIOMEDICAL APPLICATIONS

RAMESH, P.L.N., MEGANATHAN. D and P. DHASARATHAN*#

Dept.of Mechanical Engineering, Prathyusha Engineering College, Tiruvallur- 602025

*Dept. of Biotechnology, Prathyusha Engineering College, Tiruvallur- 602025

ABSTRACT

Fusion welding has traditionally been the most commonly used method for joining metals. However, in recent years, friction welding has gained significant attention due to its ability to simplify the welding process and enable the joining of metals that are otherwise difficult or impossible to weld using conventional fusion techniques. Industries such as automotive, submarine engineering, aerospace, and heavy-duty vehicle manufacturing are increasingly demanding innovative material combinations and advanced joining techniques. This study reviews various advancements and research developments in the field of friction welding, including rotary friction welding, solid-state welding, and dissimilar metal welding. Friction welding is now recognized as one of the most economical and efficient solid-state processes for producing high-strength joints between both similar and dissimilar materials. It is particularly valuable in applications where the joined materials exhibit significantly different physical and thermal properties. The process operates by converting mechanical energy into heat through relative motion between workpieces, without relying on external heat sources or electrical energy. This paper explores the fundamental aspects of friction welding, including the welding mechanism, types of relative motion, process parameters, heat generation, material deformation, microstructural evolution, and mechanical properties of the resulting joints.

Keywords: Friction welding, Dissimilar metal welding, Automotive industry, Aerospace applications, Solid-state welding, Material joining techniques

INTRODUCTION

The manufacturing technology deals with imparting the desired combination of properties to a material for performing its function. The chief manufacturing processes developed to produce

components with varying complexities includes casting, forming, machining and welding techniques. The geometry of the component, quantity and quality specifications and material properties decide the selection of a suitable manufacturing process. These techniques can be classified as additive, subtractive, and zero processes. Casting and forming are grouped as the zero processes, as they involve only shifting of metal in a controlled way from one region to another to get the required size and shape of the product. Machining is considered as subtractive process of the unwanted material from the stock is removed in the form of small chips. Welding is classified as an additive process as simple components are brought together by joining to obtain the desired shape (Amin, 1983 and Arora *et al.,* 2011).

A solid-state welding processes are characterized by the absence of melting and the formation of a narrow heat-affected zone (HAZ). In these processes, the time, temperature, and pressure are individually or in combined form to produce coalescence of the base metal without significant melting. The metallurgical properties are usually excellent and most of the processes from this family can be mechanized or automated to be used as high production rate processes (ASTM, 2006). Friction welding (FW) is a class of solid-state welding processes having significant advantages compared to the fusion welding processes such as reduced distortion and improved mechanical properties. The friction welding has 100% percent metal-to-metal joints. The various materials can be friction welded which includes nickel alloys, titanium, low and medium carbon, micro-alloyed, case hardened, corrosion-resistant, nitriding and carburizing steels (Benyounis and Olabi, 2008). FW uses low thermal energy input and causes minimal thermal degradation of the parent material. The joint undergoes hot working to form a homogenous, full surface and high integrity weld. The weld strength normally equals or exceeds the parent material strength. The principle of continuous drive FW is shown in Figure 1.

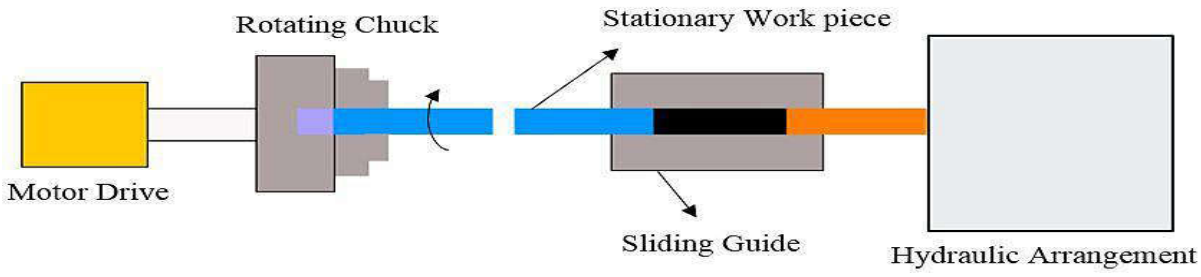

Figure 1. Schematic layout of continuous drive friction welding process

Welding of studs to plates of any thickness in applications involving marine engine valves and impeller for the turbosupercharger of a diesel engine. Thin-walled tubes can also be welded by FW to reduce overall weight requirement and material cost. Multiple parts can be welded together at a time using FW. Typical components made by friction welding include the bimetallic engine valve, brake caliper, steering shaft, conventional tubular propeller shaft, tie rod end, air brake push pad assembly, universal joint yoke, drive axle shaft, shift lever, brake "S" cam, pinion shaft, chain saw clutch drum, track roller, turbine shaft, sprocket hub, diesel injector, helicopter rotor shaft, projectile, landing gear strut, twist drill, profile cutter, lathe spindle blank, drill pipe, sucker rod, gear hub, cluster gear, rock drill piston blank, valve body and ,eccentric shaft. The materials which are friction welded during the course of research and its application's. The properties of matrix material (aluminium) and the reinforcements (silicon carbide and alumina) employed to form the metal matrix composites (MMCs) (Chowdhury *et al.,* 2010).

MATERIALS AND METHODS

The material used in this study was pre-alloyed AZ61 magnesium alloy powder and SiC particles in an equaled shape. Table 1 and Table 2 shows the chemical compositions of AZ61 and SiC used, respectively. The average particle sizes of the magnesium alloy and SiC powder were 100/m and 20/m, respectively. PA powder mixture with designed composition of 5wt% percentof SiC was mixed with as-received AZ61 pre-alloyed powder by mortar for 5 hours. To fabricate the composite sample using the hot compaction process, the mixed powder was filled in the die cavity and compressed under the pressure of 200MPa for 20 minutes at different temperature intervals, i.e 200˚C, 250˚C, 300˚C, and 350˚C. Before the compaction, the filled molded was preheated for 10 minutes with a 10kg/cm^2 gentle load. Figure shows the process flow of sample fabrication (John Wiley 2004 and Commin *et al.,* 2009). To produce AZ61/SiC metal matrix composite as-hot compacted samples, 2 gm weight of the mixed powder was filled into a cylindrical shape die cavity. The size of the as-hot compacted sample obtained was 20 mm and 4 mm in diameter and thickness, respectively to initiate a solid-state bonding of the particles, some of the samples were then sintered at temperature of 500˚C for 6 hours, under argon an atmosphere.

SiC	F.C	F.Si	Fe_2O_3	H_2O
98	0.3	0.05	0.2	0.5

Table 1: Chemical composition of AZ61 magnesiumalloy powder [mass%]

Alloy	Al	Zn	Mn	Fe	Ni	Cu	Si	Mg
AZ61	5.90	0.72	0.16	0.01	0.01	0.002	0.02	Bal.

Table 2: Chemical composition of SiC particles[mass%]

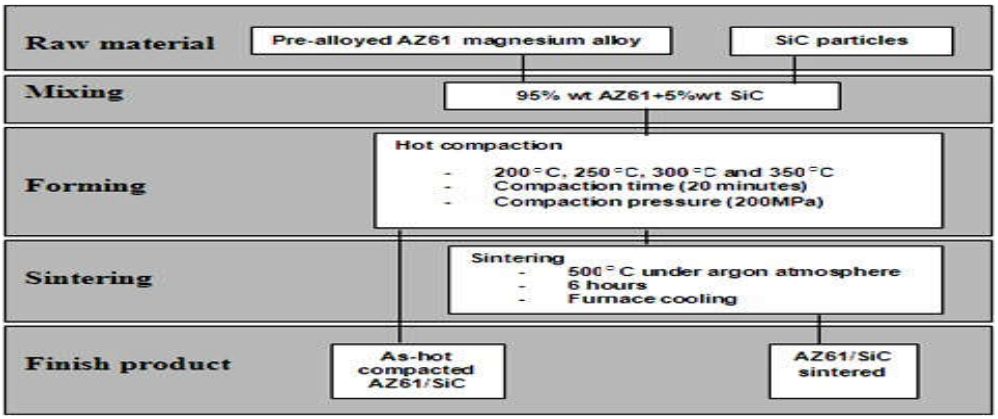

Fig. 1: Process flow of sample fabrication

The sintering was followed by furnace cooling until the samples reached the ambient temperature. The process flow of sample fabrication is shown in Fig. 1. The finish products were as-hot compacted and sintered samples. The microstructures of the finished products were then observed by optical microscopy and scan electron microscope (SEM). and instigation Ron diffraction x-ray (EDX). The etching solution used was 6g picric acid, 100 ml ethanol and 10 ml acetic acid. The hardness of the as- hot compacted and sintered samples was investigated using a Vickers hardness tester to present the hardness of bulk material.

RESULTS AND DISCUSSION

Figure 1 (a) and (b) show the SEM image received pre-alloyed AZ61 and SiC powder particles, respectively. The AZ61 particles were mostly in equiaxed shape with 100~150m in diameter and SiC particles were in equiaxed shape with 10~20m in diameter. Figure 3 shows the optical microscopy observation of as-hot compacted sample at 300°C and the one that gone through a sintering process. From the figure, it can be seen that SiC particles were fairly distributed at intervenes of matrix particles and less agglomeration occurred. It is also seen that the percentage of porosity was very small. In the as-hot compacted sample (Fig. 1(a)), presence of a lot of dislocations and defects in the matrix particles were came up into view as black dots or relatively dark area after etching. It implies that the compaction pressure used in the study was high enough to initiate inelastic deformation to the magnesium alloy powder. Furthermore, the SiC reinforcement which presence in the matrix as a second phase, acts as a

barrier for movement of dislocations so that dislocations and defects were observed in very high density in adjacent to the SiC particles. However, after the sintering process at 500°C, the black dots or dark areas were almost disappeared from the matrix particles as shown in Fig. 1(b). It is believed that the dislocations and defects that produced during the compaction process almost recovered at high temperature. The high temperature applied during the sintering process enable the dislocations moved to the low energy arrangement and significantly reduced the defects volume that results in elimination of black dots presentation. The recovery could be proved by evidenced of sub- grains, at the area closed to the SiC particle as shownin Fig. 1 (b).

At the compaction temperature of 350˚C, which was more than half of the melting temperature (T_m) of magnesium, the recovery of dislocations and defects could be observed

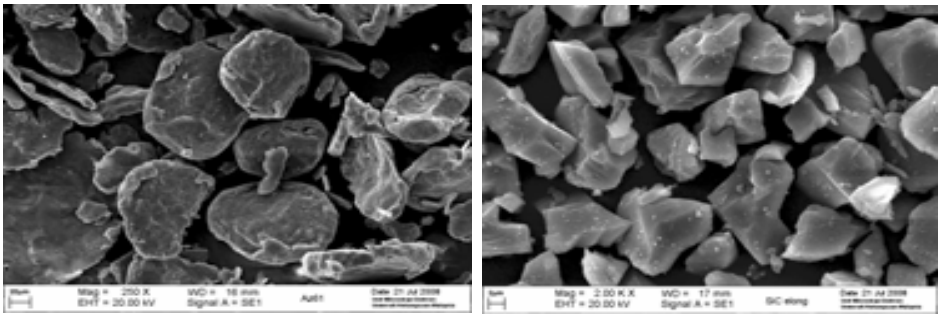

clearly as shown in Fig. 1(b), where the volume of black-dot area reduced significantly compared to the one that observed in Fig.

The temperature of 350˚C, the as hot compacted sample of AZ61/S formation of lamellar precipitates as observed. These precipitates are believed to be the $Mg_{17}Al_{12}$ phase. However, these precipitates were not observed in the AZ61 sample compacted without addition of SiC reinforcement as shown in Fig.

The particle arrangement after hot compaction at 350˚C is shown in Fig. From the figure, it is seen that the percentage of porosity is very small. This give an indication the compaction pressure is high enough to initiate plastic deformation to the powder so that the powder will arrange in most compact shape (Blawert *et al.,* 2004 andBraszczynska-Malik and Mróz, 2011). The EDX result shows the precipitates on AZ61/SiC 350°C sample contained magnesium, aluminum,oxygen and some zinc elements. The present of oxygenon the sample is expected from the process which is gone through in atmosphere environment which is the oxygen interstitially diffuse into the matrix due to its small size and its present during the SiC

heated during the process (Cai et al., 2000) and fine oxide film from powder manufacture to be dispersed as fine particles during the powder metallurgy process, playing an important role as a barrier to matrix deformation at high temperature (Mario et al., 2006). From the EDX results obtained showed high atomic percentage of oxygen on the sample, based on (William and Callister, 2000), the interstitial diffusion occurs much more rapidly compared to vacancy diffusion, its believed the process gone through by the sample were invited the oxygen to diffuse into the samples (Barnes and Fougner, 1994 and(Ben-hamu *et al.,* 2007).

Figure 2 shows the diffusion of element from SiC into AZ61 matrix. The result of EDX shows atomic percent diffusion of oxygen, carbon and silicon into the AZ61 matrix. The diffusion of those elements into the matrix may cause the saturation of magnesium, aluminium and zinc due to diffusion of silicon and carbon into the matrix. The saturation of magnesium, aluminium and zinc caused the formation of lamellar precipitates $Mg_{17}Al_{12}$. The precipitates obtained were very similar to the lamellar precipitates on AZ91D magnesium alloy. The diffusion of silicon and carbon into the matrix showed good wettability of AZ61 to SiC.

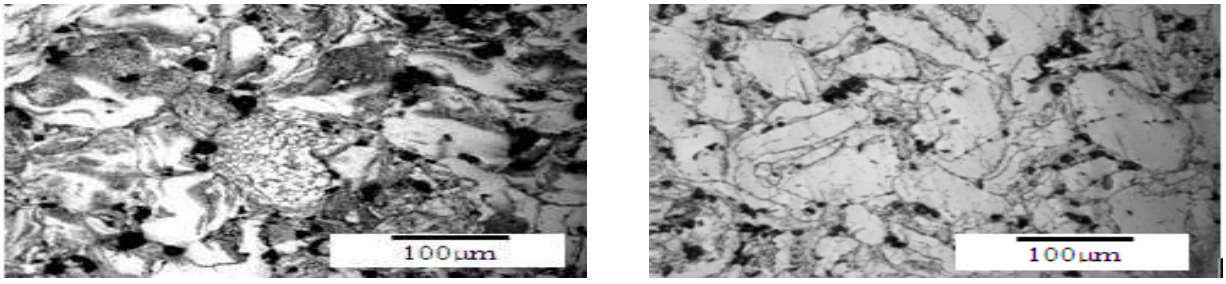

(a) As-hot compacted **(b) Sintered sample**

Fig 2. Samples obtained (a) AZ61/SiC 300°C (b)AZ61/SiC 300°C sintered (c) AZ61/SiC 350°C sinteredsample

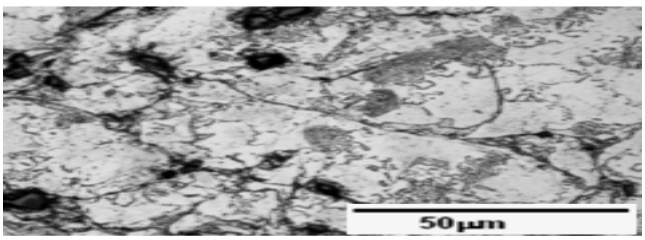

(a)

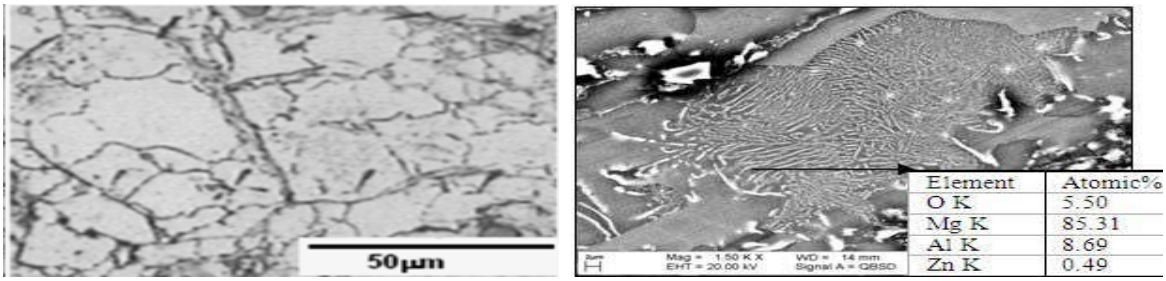

(b)

(c)

Fig 3. Microstructures of AZ61 alloy and its composites. (a) AZ61/SiC-350˚C composites, (b) AZ61 alloy compacted at 350˚C and (c) SEM image on precipitates in AZ61/SiC-350˚C composites.

The as hot compacted sample shows the variable of temperature during the compaction highly influenced the microstructure of the samples fabricated. Compaction less than half melting temperature (T_m) of magnesium alloy shows the deformation of that particles and almost none reaction of AZ61 and SiC particles. The sintered samples show the black dots are disappeared by full recovery of dislocation while the heat energy applied to allow the atomic rearrangement. In general, the grain sizes did not change much. The findings showed that the growing of the precipitates occurred during the sintering process (ASM, 1990).

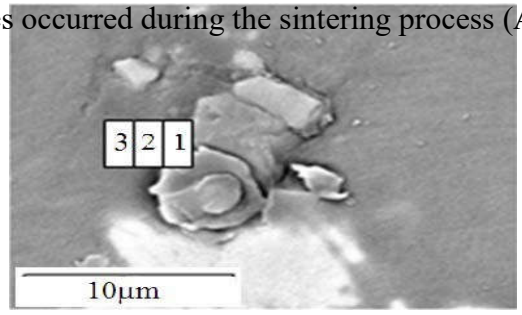

Fig. 4 Diffusion of presented elements with 1µmdistance intervals from SiC particle of AZ61/SiC 350°C sample

Hardness: Figure 3.5 shows the hardness comparison of as-hot compacted and sintered metal matrix composite samples. The result showed that the as hot compacted samples show the highest average hardness samples. The highest hardness is obtained by the as-hot magnesium alloy.

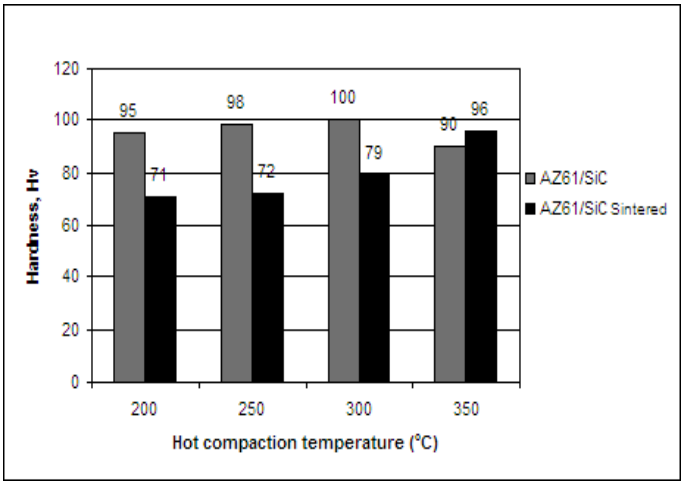

Fig 5. Hardness comparison between as-hot compactedand sintered AZ61

Compacted AZ61/SiC 300ºC sample which was 100Hv. This was due to the SiC particle on the sample was effectively act as reinforcement for AZ61 matrix. The AZ61 particles were deformed and kept internal stress due to the hot work given during the process. The presentation of SiC contributes to the high hardness value on the sample compacted at 200ºC, 250ºC and 300ºC. Sample AZ61/SiC 350ºC showed a small decreased on the hardness value which is 90Hv.Its believed that it was due to the element diffusions from SiC particles to form lamellar precipitate and the white clusters on the sample (Buffa *et al.,* 2006 and Cao. and Jahazi, 2009).

The sintered samples sintered at 500˚C for 6 hours shows full recovery dislocation energy and it resultedin the softening of the materials. The metal matrix composite sintered samples show a trend of increasing hardness value after sintering process. The highest hardness obtained by sintered sample is 96Hv for AZ61/SiC 350ºC sintered sample. The hardness value showed sintering process contributes to the extended element from SiC diffuse into AZ61 matrix. Sample AZ61/SiC 350ºC sintered showed the growing of lamellar precipitates compared to AZ61/SiC 350ºC sample. The AZ61/SiC 300ºC sample contained lot of black dots visually described the dislocation energy, but after sintering, the sample showed the grain on the sample which shows the stress release during the sintering process and resulted on the softening material. Owing to the SiC diffusion element into AZ61 matrix that was increase the formation of precipitates was increased the hardness of AZ61/SiC 350ºC sintered sample. The hardness for the AZ61/SiC 350˚C sintered sample was slightly higher compared to that of AZ61/SiC 350ºC sample (Afrin *et al.,* 2008).

FUSION WELDING PROCESS

The fusion welding process involves the partial melting and fusion of the joint between two metals. It is defined as melting together and coalescing the materials by means of heat. The thermal energy required for thesewelding operations is usually supplied by means of chemical or electrical energy. Filler metals are added to the weld area during welding. This process constitutes a major category of welding; it comprises consumables or non consumable electrode arc welding and high energy beam welding processes.

RESULTS AND DISCUSSION

Homogeneous distribution analysis: The homogeneous distribution of composite materials was analyzed and the microstructure is shown in Figure 5.1 Homogeneous distribution of silicon carbides in the matrix was observed. The microstructure of AZ61/3% SiC, AZ61/6% SiC and AZ61/9% SiC was analyzed using optical microscope.

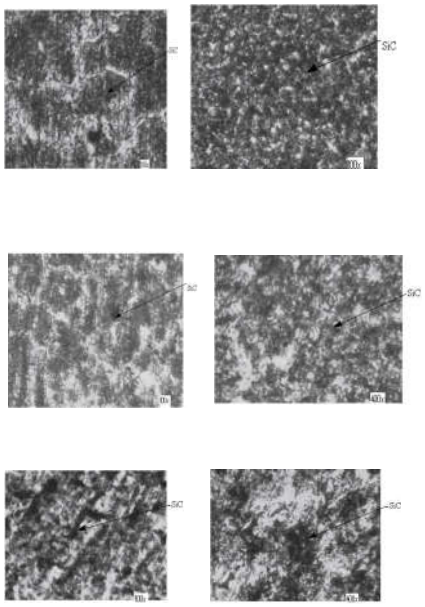

Fig 1. Homogeneous distribution of castingAZ61/SiC

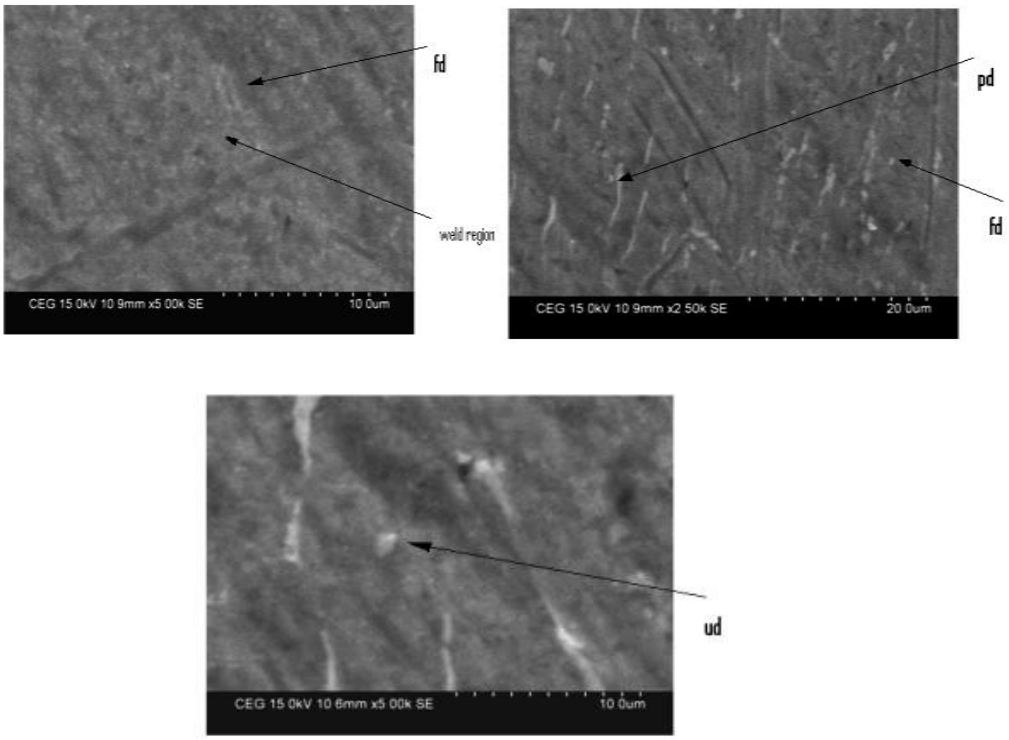

Fig 2. Microstructure analysis of AZ61/SiC 3%,6%, 9 %

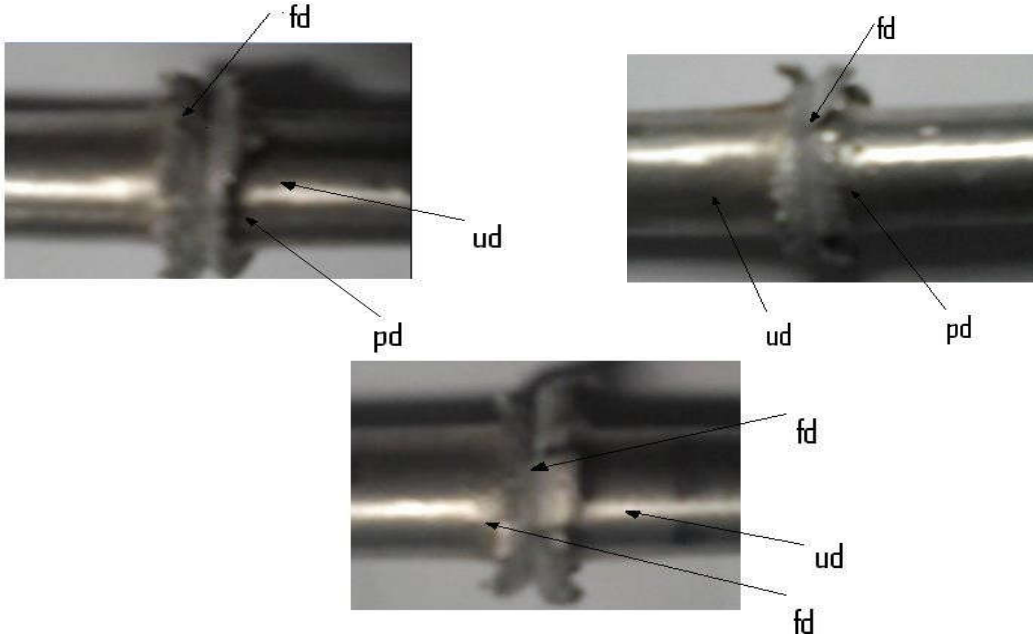

Fig 3. Macro structure of welding zone AZ61/SiC

CONCLUSION

For all welds (AZ61/3% SiC- AZ61/3% SiC, AZ61/6% SiC- AZ61/6% SiC, AZ61/9% SiC- AZ61/9% SiC) three regions differing in structure can be distinguished namely fully deformed region, partially deformed region and undeformed region. In the weld systems, partially deformed region was characterized by band distribution of reinforced particles and reduced hardness of matrix. For fully deformed region AZ61/9% SiC- AZ61/9% SiC systems hardness was lower than that in the undeformed regions. Most probably, high density reinforced particles in fully deformed region are effective to barrier dislocation moment. Hence the high density SiC particles and restriction of dislocations shift must act against annealing effect and prevent the loss of hardness in fully deformed region. The welding efficiency was increased for reduced heat affected zone. From the three zones, fully deformed zone, partially deformed and undeformed zone it was found that the reduction rate of particle size increased as the welding efficiency was increased. After micro-examination of the bonding interface, the base metal showed some second particulate formed by condensed silica particulate. However, discoloration part distributed minute silica particulate without second particulate.

REFERENCE

Afrin, N. Chen, D. L. Cao, X. and Jahazi, M. "Microstructure and tensile properties of friction stir welded AZ31B magnesium alloy Mater. Sci. Eng A., Vol. 472, pp. 179-186, 2008.

Amin. M. "Pulse current parameters for arc stability and controlled metal transfer in arc welding". Met. Construct. Vol.5 pp. 272-377, 1983.

Arora, A., A. De, and DebRoy, T. "Toward optimum friction stir welding tool shoulder diameter". Scr. Mater., Vol. 64, No. 1, pp. 9-12. 2011.

ASM Hand Book. "Magnesium and magnesium alloys", Selection and Applications, 1990.

ASTM International standard, E 112-04, "Standard test methods for determining average grain size", pp. 13-14, 2006.

Barnes, Fougner S., "Assessment of Availability of Magnesium for Automotive Applications", Spectrulite Consortium, 1994.

Ben-hamu, G., Eliezer, D., Cross, C. E. and Bollinghaus, T. H. "The relation between microstructure and corrosion behavior of GTA welded AZ31B magnesium sheet", Mater Sei Eng. A, Vol 452-453 pp. 210-218, 2007.

Benyounis, K. Y. and Olabi A G. "Optimization of different welding processes using

statistical and numerical approaches - A reference guide", Adv. Eng Software, Vol. 39, No. 6, pp. 483-496, 2008.

Blawert, C., Hort, N and Kamer, K. V. "Automotive applications of magnesium and its alloys", Trans Indian Inst Met, Vol.37, No. 4. pp. 397-408, 2004.

Braszczynska-Malik, K. N. and Mróz, M. "Gas-tungsten arc welding of A791 magnesium alloy, J. Alloys Compd. Vol. 509, No. 41, pp 9951-9958, 2011.

Buffa, G, Hua, J, Shivpuri, R. and Frasini, L. "Design of the friction stir welding tool using the continuum based FEM model". Mater. Sci Eng. A, Vol. 419, No. 1-2, pp 389-396, 2006.

Cao, X. and Jahazi, M "Effect of welding speed on the quality of friction stir welded butt joints of a magnesium alloy", Mater. Des Vol. 30, No. 6, pp 2033-2042, 2009.

Chowdhury, S. M, Chen, D. L., Bhole, S. D. and Cao, X. "Effect of pin tool thread orientation on fatigue strength of friction stir welded AZ31B-H24 Mg butt joints". Procedia Eng., Vol. 2, No. 1, 2010, pp 825-833, 2010.

Commin, L, Dumont, M., Masse, J. E and Barrallier, I "Friction stir welding of AZ31 magnesium alloy rolled sheets Influence of processing parameters", Acta Mater. Vol. 57, No. 2, pp. 326-334, 2009.

John Wiley Publications, New York, 1978. Boz Mustafa and Kurt Adem "The influence of stirrer geometry on bonding and mechanical properties in friction stir welding process Mater Des, Vol. 25, No 4, pp. 343-347, 2004.